Theor Appl Genet (2011) 122:385–394
DOI 10.1007/s00122-010-1454-y

ORIGINAL PAPER

Independent evolution of a new allele of F_1 pollen sterility gene *S27* encoding mitochondrial ribosomal protein L27 in *Oryza nivara*

Khin Thanda Win · Yoshiyuki Yamagata · Yuta Miyazaki · Kazuyuki Doi · Hideshi Yasui · Atsushi Yoshimura

Received: 12 June 2010 / Accepted: 8 September 2010 / Published online: 28 September 2010

Abstract Loss of function of duplicated genes plays an important role in the evolution of postzygotic reproductive isolation. The widespread occurrence of gene duplication followed by rapid loss of function of some of the duplicate gene copies suggests the independent evolution of loss-of-function alleles of duplicate genes in divergent lineages of speciation. Here, we found a novel loss-of-function allele of *S27* in the Asian annual wild species *Oryza nivara*, designated *S27-niv*^{s}, that leads to F_1 pollen sterility in a cross between *O. sativa* and *O. nivara.* Genetic linkage analysis and complementation analysis demonstrated that *S27-niv*^{s} lies at the same locus as the previously identified *S27* locus and *S27-niv*^{s} is a loss-of-function allele of *S27*. *S27-niv*^{s} is composed of two tandem *mitochondrial ribosomal protein L27* genes (*mtRPL27a* and *mtRPL27b*), both of which are inactive. The coding and promoter regions of *S27-niv*^{s} showed a number of nucleotide differences from the functional *S27-T65*$^+$ allele. The structure of *S27-niv*^{s} is different from that of a previously identified null *S27* allele, *S27-glum*^{s}, in the South American wild rice species *O. glumaepatula*, in which *mtRPL27a* and *mtRPL27b* are absent. These results show that the mechanisms for loss-of-function of *S27-niv*^{s} and *S27-glum*^{s} are different. Our results provide experimental evidence that different types of loss-of-function alleles are distributed in geographically and phylogenetically isolated species and represent a potential mechanism for postzygotic isolation in divergent species.

Communicated by E. Guiderdoni.

Electronic supplementary material The online version of this article (doi:10.1007/s00122-010-1454-y) contains supplementary material, which is available to authorized users.

K. T. Win · Y. Yamagata · Y. Miyazaki · K. Doi · H. Yasui · A. Yoshimura (✉)
Plant Breeding Laboratory, Faculty of Agriculture, Kyushu University, 6-10-1 Hakozaki, Higashi-ku, Fukuoka 812-8581, Japan
e-mail: ayoshi@agr.kyushu-u.ac.jp

Present Address:
K. Doi
Graduate School of Bioagricultural Sciences, Nagoya University, Chikusa, Nagoya 464-8601, Japan

Introduction

Gene duplication provides opportunities to increase gene diversity during evolution. Because the original function supplied from one gene copy allows the other copy to escape elimination through selection, duplicate genes allow the accumulation of mutations that introduce a new function (neo-functionalization), divide the original function (sub-functionalization), or cause loss of function (non-functionalization) (Lynch and Force 2000). Recent studies have demonstrated that duplicate genes contribute to reproductive isolation, which generally prevents gene flow between species, and they play an important role in plant speciation (Rieseberg and Willis 2007). For example, the neo-functionalized duplicate gene *Odysseus-site Homeobox* (*OdsH*) causes postzygotic reproductive isolation in *Drosophila* (Sun et al. 2004). Similarly, non-functionalization has contributed to a passive type of postzygotic reproductive isolation through reciprocal loss of duplicate genes between two divergent species; when this occurs, selection against hybrids may occur in either a sporophytic (zygotic) or gametophytic (gametic) manner (Bikard et al. 2009; Yamagata et al. 2010). Genome-wide analysis has shown a very high rate of gene duplication and a rapid loss of most duplicate genes within a few million years (Lynch and

Conery 2000). It has been suggested that loss-of-function mutations at the same locus in different species have evolved independently and contribute to reproductive isolation (Lynch and Force 2000). However, this has not yet been demonstrated.

The two cultivated species of rice (*Oryza sativa* and *O. glaberrima*) and six wild species are classified into the AA-genome species in the genus *Oryza* (Khush 1997). Exchange of genes among the AA-genome species can be accomplished by conventional interspecific hybridization and recombination. However, F_1 pollen sterility is frequently observed in these hybrids and prevents the transfer of useful genetic resources from wild species to cultivated rice. The genetic mechanism of hybrid sterility has been extensively studied in rice, and several F_1 pollen sterility loci have been reported (Doi et al. 2008; Koide et al. 2008). The genetic mechanisms of F_1 hybrid sterility have been explained using two genetic models: the one-locus allelic interaction model and the two-locus epistatic interaction model (Oka 1988). Recognition of the genetic models has been based on segregation patterns of sterility as "Mendelian" loci. Gametophytic F_1 embryo sac sterility fitting the one-locus allelic interaction model was recently characterized by gene cloning of *S5* encoding aspartic protease (Chen et al. 2008). *S5* is caused by aberrant interaction of protein products of the *S5-i* and *S5-j* alleles derived from a single genomic locus in rice. Similarly, *Sa* has been recognized as a single Mendelian locus for the one-locus allelic interaction causing gametophytic F_1 pollen sterility in rice. However, *Sa* was resulted from interaction of three alleles derived from two adjacent genomic loci in rice (Long et al. 2008), which is controlled by different genetic architecture from *S5* although *Sa* and *S5* have been recognized as the one-locus allelic interaction model. Hybrid sterility caused by interaction between disharmonious alleles from two or more loci, like the case of *Sa*, fit to the Bateson–Dobzhansky–Muller (BDM) incompatibility model, which is widely accepted in various plant and animal species (Coyne and Orr 2004). Recently, a case of gametophytic BDM incompatibility caused by the epistatic interaction between the two complementary loci has been demonstrated (Yamagata et al. 2010): reciprocal loss of duplicate genes on chromosomes 4 (*S28* locus) and 8 (*S27* locus) caused hybrid sterility in the F_1 between allopatric species, *Oryza sativa* [*japonica* cultivar Taichung 65 (T65)] and *O. glumaepatula* (accession number IRGC105668). *S27* and *S28* are duplicate loci encoding mitochondrial ribosomal protein L27 (mtRPL27), which is required for normal pollen development. The *O. glumaepatula* allele at *S27* (*S27-glum*^{s}) and the T65 allele at *S28* (*S28-T65*^{s}) no longer function as *mtRPL27* genes, and pollen grains carrying both of these alleles are sterile (as indicated by a superscript "*s*"). Meanwhile, the T65 allele at *S27* (*S27-T65*$^+$) and the *O. glumaepatula* allele at *S28* (*S28-glum*$^+$) encode normal mtRPL27 protein, and pollen grains carrying at least one of these fertile alleles are fertile (as indicated by a superscript "+"). Duplication of *mtRPL27* at *S27* and *S28* was caused by segmental duplication of an approximately 30-kb genomic sequence (containing *mtRPL27*) from chromosome 4 to chromosome 8. The loss of function of *S27-glum*^{s} is due to the absence of the 30-kb segment. The duplicated segment on chromosome 8 was found in all investigated accessions of *O. sativa*, Asian wild annual species *O. nivara*, and perennial species *O. rufipogon* (Yamagata et al. 2010). However, it is unknown whether loss-of-function alleles exist in accessions of the Asian AA-genome species carrying duplication of *mtRPL27* genes on chromosomes 4 and 8.

Here, we identified a new allele of *S27*, *S27-niv*^{s}, on chromosome 8, in hybrids between *O. nivara* and T65. The pollen grains carrying the *O. nivara* allele of *S27* (*S27-niv*^{s}) were sterile. Complementation analysis demonstrated that the *S27-niv*^{s} allele is a loss-of-function allele of *S27*. In addition, we determined the genomic sequence of the *mtRPL27* gene region in *S27-niv*^{s} and acquired experimental evidence for an independent origin of this loss-of-function allele at *S27* locus.

Materials and methods

Plant materials

Introgression lines (ILs) containing chromosome segments of the Asian annual wild rice *O. nivara* (the donor parent) in an *O. sativa* genetic background were generated. A cultivar of Asian cultivated rice (*O. sativa* L. ssp. *japonica* 'Taichung 65'; designated T65) was used as the female parent in crosses with *O. nivara* (accession number IRGC105444; Sri Lanka) to produce F_1 plants with T65 cytoplasm. These F_1 plants were successively backcrossed with T65 as the male parent. During the development of ILs using marker-assisted selection (MAS), segregation of pollen sterility was observed in BC_4F_1 populations that carried an *O. nivara* segment of chromosome 8. ILs heterozygous for that segment of chromosome 8 were screened in the BC_4F_1 generation to identify the pollen sterility gene, and their progeny in the BC_4F_3 generation was used for high-resolution linkage analysis.

DNA extraction and genotyping using SSR markers

Genomic DNA for linkage analysis using simple sequence repeat (SSR) markers was extracted from freeze-dried leaf samples according to Dellaporta et al. (1983), with minor modifications. PCR reactions were performed in 15 µl of

reaction mixture containing 50 mM KCl, 10 mM Tris–HCl (pH 9.0), 1.5 mM $MgCl_2$, 200 μM each dNTP, 0.2 μM each primer, 0.75 units *Taq* polymerase (Takara, Otsu, Japan), and approximately 25 ng template DNA in a GeneAmp PCR system 9700 (Applied Biosystems, Foster City, CA, USA). The PCR program used was 95°C for 5 min, followed by 35 cycles of 95°C for 30 s, 55°C for 30 s and 72°C for 30 s. PCR products were run in 4% agarose gels (Agarose HT; Amresco Inc., Solon, OH, USA) in 0.5× TBE buffer.

Evaluation of pollen fertility

Panicles at flowering stage were fixed and stored in 70% (v/v) ethanol. For each sample, pollen grains from six anthers in a single spikelet collected a few days before anthesis were stained with 1% iodine–potassium iodide (I_2–KI) solution on a glass slide. More than 200 pollen grains per slide were evaluated for pollen fertility under an Axioplan light microscope (Zeiss, Jena, Germany). Pollen grains that were morphologically the same as grains of T65 were scored as normal; empty, unstained, incompletely stained, or small grains were scored as sterile.

Observation of postmeiotic pollen development

Panicles in the meiotic to mature stages were continuously collected to observe pollen development from the unicellular to mature stages. Panicles were fixed in fixative solution containing 4% (w/v) paraformaldehyde, 0.25% (w/v) glutaraldehyde, 0.02% (v/v) Triton X-100, and 100 mM sodium phosphate (pH 7.5) at 4°C for 24 h. After rinsing in 100 mM sodium phosphate buffer, the fixed panicles were stored in 100 mM sodium phosphate buffer containing 0.1% (w/v) sodium azide (NaN_3). The hematoxylin staining procedure of Chang and Neuffer (1989) was used with minor modifications.

Evaluation of germination ability and viability of pollen

To evaluate pollen germination on artificial medium, pollen just after flowering in natural conditions was shed onto a glass microscope slide containing a drop of germination medium [15% (w/v) sucrose, 0.01% (w/v) H_3BO_3, 0.03% (w/v) $CaCl_2$ and 0.6% (w/v) gellan gum]. After 6–8 min incubation at room temperature, the pollen grains were observed and photographed under a light microscope.

To evaluate the viability of pollen grains by the fluorochromatic reaction (FCR) test, panicles at the heading stage were collected and fresh pollen at a few days before anthesis was stained with 0.05 mM fluorescein diacetate (FDA) solution. The stained samples were observed immediately under a fluorescence microscope with a 450–490-nm exciter filter and a 525-nm emission filter according to Heslop-Harrison and Heslop-Harrison (1970).

Linkage analysis

To perform linkage analysis of the pollen sterility gene from IRGC105444, we analyzed the BC_4F_3 population derived from a BC_4F_2 plant that was heterozygous for IRGC105444 segment on chromosome 8 and homozygous for IRGC105444 segments on chromosomes 6 and 7 (Fig. 1a). Three SSR markers on chromosome 8, *RM1309* and *RM8264* (McCouch et al. 2002) and *M1_S27* (Table 1), were used in the linkage analysis. Recombination values between markers were estimated using the maximum-likelihood equation (Allard 1956) and transformed into genetic map distances (cM) using Kosambi's mapping function (Kosambi 1944). To further define the map position of *S27-niv*^{s}, the SSR markers *S27_ssr1*, *S27_ssr8* and *M1_S27* (Table 1), and *RM8264* were used in high-resolution mapping of the BC_4F_3 population.

Complementation analysis

To confirm that the sterility of pollen grains carrying *S27-niv*^{s} allele is caused by a defect in *mtRPL27*, a genomic DNA fragment containing a functional copy of *mtRPL27a* isolated from the fertile allele *S27-T65*$^+$ (*Sma*I fragment in Fig. 3b) was introduced into semi-sterile plants (*S27-T65*$^+$/*S27-niv*^{s}, *S28-T65*^{s}/*S28-T65*^{s}) by *Agrobacterium*-mediated transformation (Hiei et al. 1994). The *Sma*I fragment was cloned into the Ti-plasmid binary vector pPZP2H-lac (Fuse et al. 2001). The T_0 plants were grown to maturity in a temperature- and humidity-controlled greenhouse for transgenic plants. Spikelets were collected a few days before flowering, fixed, and stored in 70% (v/v) ethanol, and pollen fertility was evaluated as described above.

Molecular cloning of the genomic DNA sequence of *S27-niv*^{s}

The presence or absence of a 30-kb duplicated segment at *S27* locus was determined using PCR markers *S27D* and *S27ND*, respectively (Yamagata et al. 2010; Table 1). To determine the genomic sequence of the *S27-niv*^{s} allele, genomic DNA fragments of IRGC105444 around the *mtRPL27* gene region on chromosome 8 were amplified with KOD-Plus DNA polymerase and cloned into the pTA2 vector (Toyobo, Osaka, Japan). Four overlapping *O. nivara* genomic clones (NGC1-4) were obtained by amplification using primer pairs *M2_S27* for NGC1, covering the *mtRPL27a* promoter region; *M3_S27* for NGC2, covering the coding region of *mtRPL27a* and the promoter region of

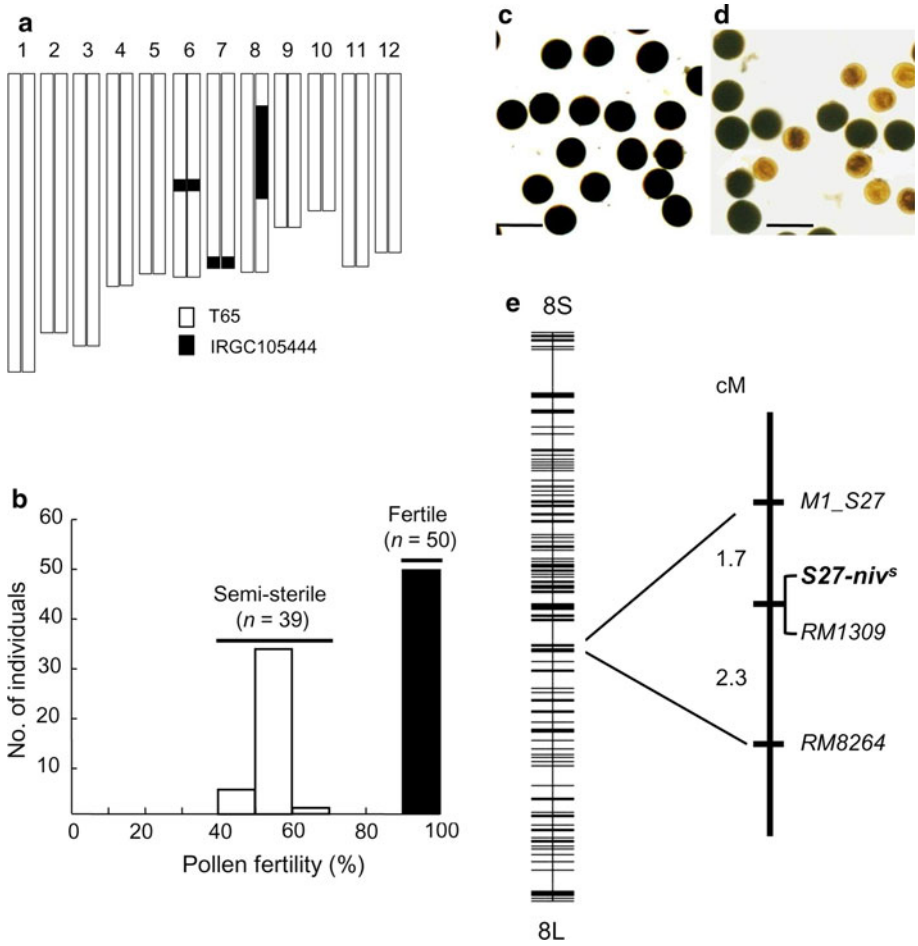

Fig. 1 Identification of *S27-niv*^{s}, a pollen sterility gene on chromosome 8. **a** Graphical genotype of the BC_4F_2 plant used to generate the mapping population (BC_4F_3). **b** Frequency distribution of pollen fertility classified by the genotypes of SSR marker *RM1309* in the BC_4F_3 population. *Black bars* and *white bars* represent T65 homozygotes and heterozygotes, respectively. IRGC105444 homozygous plants did not segregate in this population because of sterility of pollen grains carrying the *S27-niv*^{s} allele. **c, d** Pollen grains of fertile (**c**) and semi-sterile (**d**) plants stained with I_2–KI. Scale bars = 50 µm. **e** Linkage map showing the location of *S27-niv*^{s}. *Left* latest high-density RFLP framework map from the Rice Genome Research Program (RGP); available at http://rgp.dna.affrc.go.jp/publicdata/geneticmap2000/index.html. *Right* location of *S27-niv*^{s} with respect to SSR markers used in this study

Table 1 PCR primers used in this study

Marker	Purpose	Forward primer sequence (5′–3′)	Reverse primer sequence (5′–3′)
M1_S27	SSR marker	GACAAGTTTGCTGTTGTCAACG	TCAGATCAAGTTGAATTCAAGCA
S27_ssr1	SSR marker	ATGCGAAGGCAATGAAAAAG	TGAAGCACAACGCTAACAGAG
S27_ssr8	SSR marker	CTCGATGGTAGATTGGGGTA	CATCTGTTCGCTGCTCTGTT
S27D	STS marker	TTGAATTCCGAGAGTCTGGC	GGTCGTCGGAGTGGTAGACGAAG
S27ND	STS marker	GGTCGTCGGAGTGGTAGACGAAG	TGTTCACCAAATGACTCCAAATCG
M2_S27	Cloning of NGC1	ACGGCAGGTGTTTAAGGTCTTTGGATG	CTCACGCAATTCATGGATTGCTGAAGA
M3_S27	Cloning of NGC2	AGCCTTTCAATCCAGAAACCTCAGGGG	TCCATTCCCGTAAACCCTAAAATGGCC
M4_S27	Cloning of NGC3	CAAACGATGGGGGCCTTAGTTTGTTCA	CCTCTCCTGAAAACTGATGAAAAAGCC
M5_S27	Cloning of NGC4	GCTGGAATTAGGCTGACCAAATCCTTG	CCAGGGTAGATTCCAAAATGTGAAGAG
M6_S27	SNP marker	CCCAAGTGGCCAAATACCTAATTCCTC	CTTGTATTTTGCAGCCGTCGGGCTAA
M7_S27	InDel marker	CCGAATCCGGGCCGTCCATT	ATCTCTCCCGCGCCCAGA ACGA
M8_S27	SNP marker	AGTGATTCGACCCCTGCAGCTGAACTA	AATTCAACCCAGAAGCCTCTTAATCGCA

SSR simple sequence repeat, *STS* sequence-tagged-site, *SNP* single nucleotide polymorphism, *InDel* polymorphism of PCR bands due to insertion/deletion of each allele

mtRPL27b; *M4_S27* for NGC3, covering the promoter region of *mtRPL27b*; and *M5_S27* for NGC4, covering the coding region of *mtRPL27b* (Table 1; Fig. 4a). Sequences of the inserted DNA fragments were determined by cycle sequencing using BigDye Terminator v3.1 (Applied Biosystems, Foster City, CA, USA).

To confirm whether the obtained NGC clones were correctly amplified from *S27* rather than from *S28*, three

S27-niv^s allele-specific dominant markers, *M6_S27*, *M7_S27*, and *M8_S27*, which amplify DNA fragments from the genomic regions corresponding to NGC1, NGC2 and NGC3, and NGC4 at *S27-niv*^{s}, respectively, were developed (Table 1). The *M6_S27* and *M8_S27* markers were designed to amplify only the DNA fragments from *S27-niv*^{s} allele, but not to amplify from *S27-T65*$^+$ and *S28-T65*^{s} alleles (Table S1). The *M7_S27* marker was designed to amplify DNA fragments from all three alleles with different sizes of DNA fragments (Table S1). In co-segregation analysis of the four clones at the *S27* locus, BC_4F_3 plants derived from a BC_4F_2 plant heterozygous at *S27* (*S27-T65*$^+$/*S27-niv*^{s}) and T65 homozygous at *S28* (*S28-T65*^{s}/*S28-T65*^{s}) were scored for three *S27-niv*^{s} allele-specific dominant markers.

The sequences reported in this paper were deposited in the DNA Data Bank of Japan [accession numbers AB496673 (*mtRPL27a S27-T65*$^+$), AB496674 (*mtRPL27b S27-T65*$^+$) and AB576647 (*mtRPL27a S27-niv*^{s} and *mtRPL27b S27-niv*^{s})].

Results

Identification of a pollen sterility gene on chromosome 8

The rice lines T65 (*O. sativa*) and IRGC105444 (*O. nivara*) each showed more than 90% pollen fertility, but their F_1 hybrids showed approximately 25% pollen fertility. The genome-wide genetic analysis of the F_1 pollen sterility in hybrid progeny between *O. sativa* and *O. nivara* revealed that *S36* on chromosome 12 and *q*PS1 on chromosome 1 contributed to pollen sterility in this hybrid (Win et al. 2009). In the process of generating a series of ILs of *O. nivara* chromosome segments in a T65 genetic background, pollen sterility was observed in some individuals from the BC_4F_1 population that carried an *O. nivara* segment of chromosome 8 in the heterozygous state. By linkage analysis in a BC_4F_3 population developed from a BC_4F_2 plant (Fig. 1a) carrying *O. nivara* segments of chromosomes 6, 7, and 8, we determined that the gene controlling pollen sterility lies on chromosome 8. The BC_4F_3 population (n = 89) exhibited a clear bimodal distribution of pollen fertility, with 39 semi-sterile and 50 fertile plants (Fig. 1b). Pollen fertility of the fertile plants was greater than 90% (Fig. 1b, c), whereas that of semi-sterile plants ranged from 40.5 to 56.8%, with an average of 49.2% (Fig. 1b, d). The sterile pollen grains produced by semi-sterile plants were unstained by the I_2–KI staining solution. All of the fertile plants were T65 homozygotes, whereas all semi-sterile plants were heterozygotes, based on the genotype at the SSR marker *RM1309* (Fig. 1b) in this population. This result suggests that the pollen sterility gene was tightly linked to *RM1309* on chromosome 8 and caused heterozygous plants to exhibit semi-sterility. No plants homozygous for the IRGC105444 segment were observed in the mapping population; this segregation distortion was considered to result from sterility of pollen grains carrying the allele from the IRGC105444 parent. The observed segregation ratio of the fertile and semi-sterile plants fits the theoretical 1:1 ratio (χ^2 = 1.36, P = 0.24) expected for gametophytic pollen sterility under the control of a single nuclear gene.

Linkage analysis showed that the pollen sterility gene co-segregated with the marker *RM1309* and was located between *M1_S27* and *RM8264*, at distances of 1.7 and 2.3 cM, respectively (Fig. 1e). In this same chromosomal region, an *S27* locus conferring gametophytic F_1 pollen sterility had previously been found in hybrids between T65 and *O. glumaepatula* (Yamagata et al. 2010). In the progeny of that cross, pollen grains carrying both the *S27-glum*^{s} and *S28-T65*^{s} alleles were sterile, so plants heterozygous at *S27* (*S27-T65*$^+$/*S27-glum*^{s}) and homozygous for the *S28* non-functional allele from T65 (*S28-T65*^{s}/*S28-T65*^{s}) showed pollen semi-sterility. Here, semi-sterile plants were heterozygous at *RM1309* and homozygous for chromosome 4 from T65, which carries *S28-T65*^{s} (Fig. 1a). This result was similar to that of the T65 × *O. glumaepatula* cross; so we speculated that the allele identified here lies at the same locus as the previously identified *S27* locus, and designated it *S27-niv*^{s}. Since the pollen grains carrying the IRGC105444 allele showed sterility, the IRGC105444 allele was named as the sterile allele (*S27-niv*^{s}), and the T65 allele was named as the fertile allele (*S27-T65*$^+$).

To examine the morphological and developmental features of the sterile pollen, pollen development in postmeiotic stages was investigated in *S27-niv*^{s} semi-sterile plants using the I_2–KI and hematoxylin staining methods. No phenotypic abnormality was observed during the unicellular stages. At the bicellular stage, we detected generative and vegetative cells in all pollen grains (Fig. 2a, b), but half of the pollen grains failed to initiate starch accumulation (Fig. 2c). At the mature stage, almost half of the pollen grains looked normal, carrying one vegetative cell and two sperm cells (Fig. 2d), but the remainder were mainly at the bicellular stage and had not accumulated starch (Fig. 2e, f). These results reveal that the development of sterile pollen grains caused by *S27-niv*^{s} was arrested at the bicellular stage before initiation of starch accumulation, similar to the sterile pollen grains caused by *S27-glum*^{s} (Yamagata et al. 2010). In vitro pollen germination tests revealed no germination of any of the morphologically abnormal pollen grains in *S27-T65*$^+$/*S27-niv*^{s} heterozygous plants (Fig. 2g), whereas about 90% of pollen from T65 parent germinated (Fig. 2h). In addition, pollen viability testing by FCR in pollen grains at a few days before anthesis showed a positive green fluorescence signal in both fertile and sterile pollen grains due to the endogenous esterase activity of

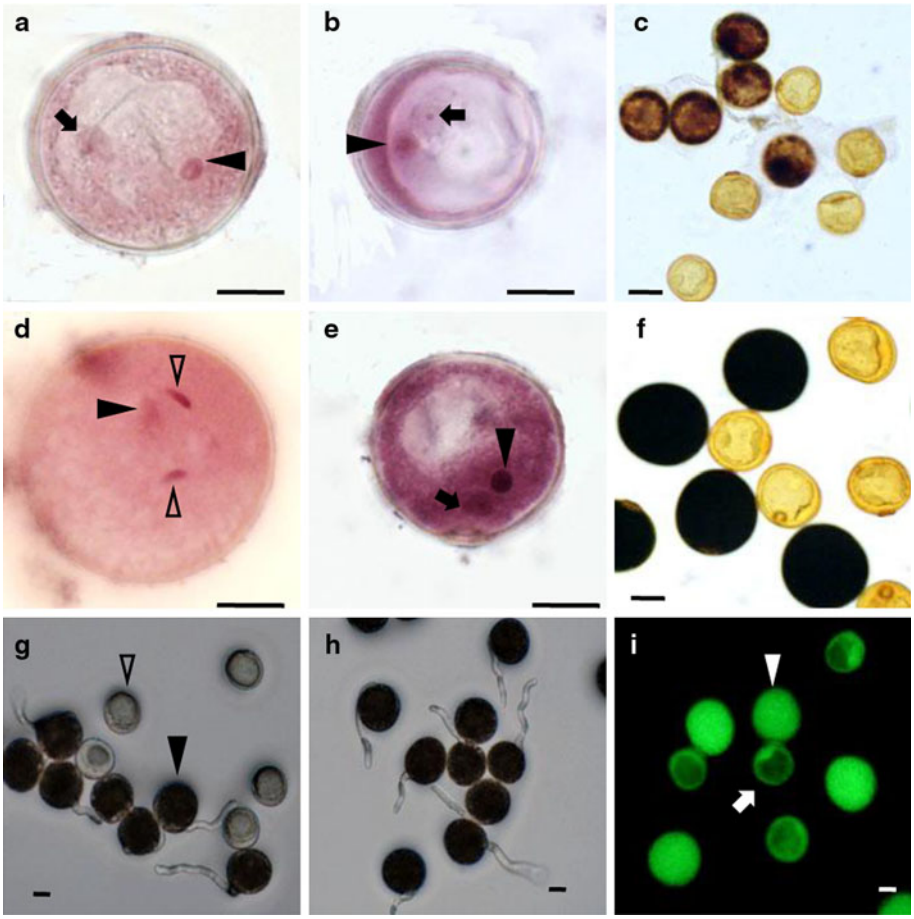

Fig. 2 Characterization of sterile pollen grains caused by *S27-niv*^{s}. **a–f** Light-microscopic observation of postmeiotic pollen development in bicellular (**a–c**) and mature (**d–f**) stages in terms of nuclei by hematoxylin staining (**a, b, d, e**) and starch accumulation by I_2–KI staining (**c, f**). **a, b, d, e** Individual normal (**a, d**) and sterile (**b, e**) pollen grains. *Black arrowheads*, *white arrowheads*, and *black arrows* indicate nuclei of vegetative cells, sperm cells, and generative cells, respectively. **g, h** Evaluation of pollen germination ability on artificial medium for *S27-niv*^{s} heterozygous semi-sterile plant (**g**) and T65 parent (**h**). *Black arrowheads* and *white arrowheads* indicate fertile and sterile pollen grains, respectively. **i** Fluorescence microscopic observation of the viability of pollen in fluorescein diacetate (FDA) staining solution. *White arrowhead* and *white arrow* indicate fertile and sterile pollen grains, respectively. *Scale bars* = 10 μm

individual pollen grains (Fig. 2i), and fainter signals which correspond to vacuoles in the center of sterile pollen grains (Fig. 2i). These results indicate that sterile pollen grains caused by *S27-niv*^{s} retained their viability but lost their germination ability because of developmental arrest at the bicellular stage and lack of starch accumulation.

High-resolution linkage analysis of *S27-niv*^{s}

To narrow down the genomic region containing the *S27-niv*^{s} locus, we performed high-resolution linkage analysis using 1,145 plants of the BC_4F_3 populations derived from the BC_4F_2 plants that were heterozygous (*S27-T65*$^+$/*S27-niv*^{s}) at *S27* and T65 homozygous (*S28-T65*^{s}/*S28-T65*^{s}) at *S28*. The high-resolution mapping narrowed the *S27-niv*^{s} candidate region to 122.2 kb on the Nipponbare reference genome between markers *S27_ssr1* and *S27_ssr8*, with one and two plants, respectively, carrying recombination between phenotype and genotype of each marker (Fig. 3a). This candidate region included the gene duplication at the *S27* locus (*mtRPL27a* and *mtRPL27b*). Therefore, we concluded that *S27-niv*^{s} lies at the same locus as the previously identified *S27* locus on chromosome 8.

Complementation analysis

In the cross of T65 × *O. glumaepatula*, sterility of pollen grains is caused by the sterile alleles *S27-glum*^{s} and *S28-T65*^{s}, both of which are loss-of-function alleles of *mtRPL27* (Yamagata et al. 2010). Since sterile pollen grains here carried *S27-niv*^{s} and *S28-T65*^{s}, we speculated that the sterile allele *S27-niv*^{s} is also a loss-of-function allele. Therefore, we expected that introduction of a functional *mtRPL27* gene would rescue the fertility of pollen grains carrying *S27-niv*^{s} and *S28-T65*^{s}. To test this expectation, we performed complementation analysis by transforming a genomic DNA fragment containing a wild-type *mtRPL27a* gene (a *Sma*I fragment derived from the fertile allele *S27-T65*$^+$; Fig. 3b) into semi-sterile plants carrying *S27-T65*$^+$/*S27-niv*^{s} and *S28-T65*^{s}/*S28-T65*^{s}. If the introduced *mtRPL27a* gene were able to rescue the fertility of pollen grains carrying *S27-niv*^{s} and *S28-T65*^{s}, we would expect most T_0 plants carrying one copy of the transgene to show 75% pollen fertility, because 75% of the pollen grains would contain the *S27-T65*$^+$ allele or the transgene, or both. Linkage of the transgene and *S27* could result in altered fertility percentages in some T_0 plants. Pollen fertility of the T_0 transgenic plants transformed with the *Sma*I fragment ranged from 53

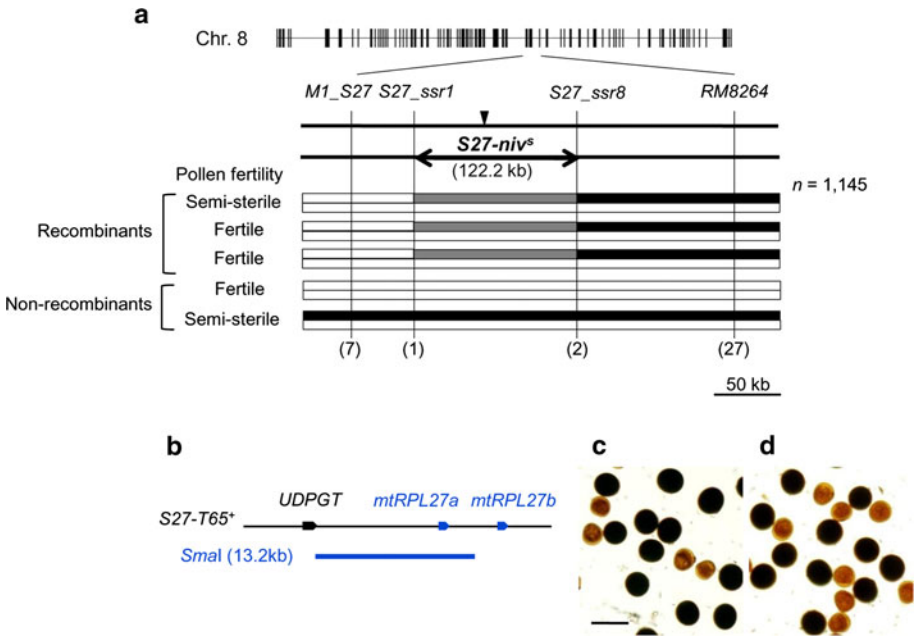

Fig. 3 High-resolution linkage and complementation analyses of *S27-niv*^{s}. **a** High-resolution linkage analysis of *S27-niv*^{s}. The RFLP framework map was obtained from the latest high-density rice genetic map from RGP (http://rgp.dna.affrc.go.jp/publicdata/geneticmap2000/index.html). Pollen fertility and graphical genotypes of the three informative plants for the high-resolution mapping with recombination and those of the typical plants without recombination are shown. Numbers of recombinants between the genes and markers are indicated in *parentheses*. *White boxes* and *black boxes* indicate T65 and IRGC105444 chromosomal segments, respectively. Recombination regions are illustrated by *gray boxes*. *Black arrowhead* indicates the location of the *mtRPL27a* and *mtRPL27b* genes found in the rice reference sequence of Nipponbare. **b–d** Complementation analysis. *S27-niv*^{s} plants were transformed with a *Sma*I restriction fragment containing *mtRPL27a* derived from the functional allele *S27-T65*$^+$. **b** Location of the *Sma*I restriction fragment used in the complementation analysis. **c, d** Pollen grains of T_0 plants transformed with the *Sma*I fragment (**c**) or empty vector (**d**) stained with I_2–KI solution. *Scale bar* = 50 μm

to 86%, with most plants in the 70–80% category (Table 2; Fig. 3c). On the other hand, transgenic plants transformed with the empty vector never showed more than 56% pollen fertility (Table 2; Fig. 3d). This result demonstrates that the *mtRPL27a* gene in the *Sma*I fragment rescued the sterility of *S27-niv*^{s} *S28-T65*^{s} pollen grains, confirming that the sterility of pollen grains carrying *S27-niv*^{s} allele is caused by a defect in *mtRPL27*.

Molecular cloning of the genomic DNA sequence of *S27-niv*^{s}

The *S27* locus in T65 is composed of two tandem copies of the *mtRPL27* gene (*mtRPL27a* and *mtRPL27b*), both of which encode functional mtRPL27 protein. *S27-glum*^{s} is a loss-of-function allele caused by the absence of a 30-kb duplicated segment at *S27* locus including both *mtRPL27* gene copies (Yamagata et al. 2010). In *O. nivara* accession IRGC105444, we detected the existence of a 30-kb duplicated segment at *S27* locus using two PCR markers, *S27D* and *S27ND*, which detect the presence and absence, respectively, of the duplicated segment (Fig. S1). This result indicates that the structures of *S27-glum*^{s} and *S27-niv*^{s} are different, so the cause of loss-of-function of *S27-niv*^{s} is likely to be different from that in *S27-glum*^{s}.

Therefore, to determine the genomic sequence of the *S27-niv*^{s} allele, we obtained the four overlapping *O. nivara* genomic clones: NGC1, NGC2, NGC3 and NGC4, which amplified from total genomic DNA of IRGC105444 using primers specific for *mtRPL27a* and *mtRPL27b* at *S27* locus (Fig. 4a). To confirm whether the obtained NGC clones were correctly amplified from *S27*, rather than from *S28*,

Table 2 Distribution of pollen fertility (%) in heterozygous *S27-T65*$^+$/*S27-niv*^{s} T_0 plants transformed with a functional copy of *mtRPL27a*

Restriction fragment	Transgene	Allele	No. of plants										Total
			0–10	10–20	20–30	30–40	40–50	50–60	60–70	70–80	80–90	90–100	
*Sma*I	*mtRPL27a*	*S27-T65*$^+$	0	0	0	0	0	3	1	10	4	0	18
Empty vector	–	–	0	0	0	0	5	3	0	0	0	0	8

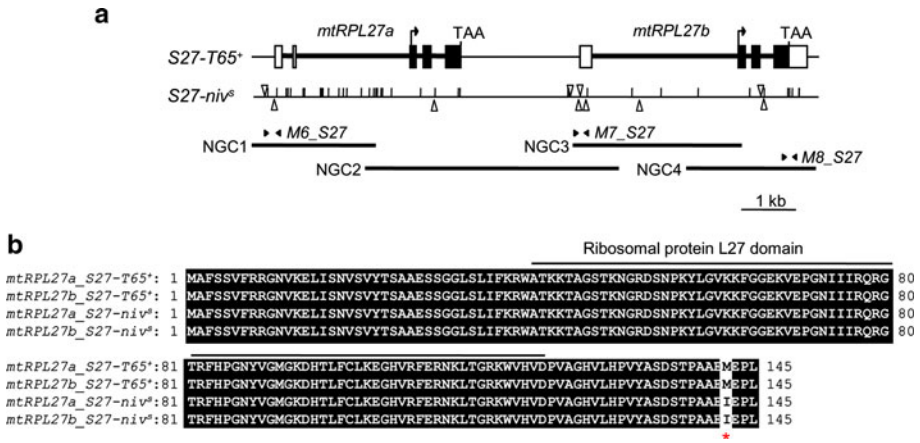

Fig. 4 Molecular cloning of the genomic DNA sequence of *S27-niv*^{s}. **a** The genomic DNA structure of T65 and IRGC105444 around the *S27* locus on chromosome 8. Introns, non-coding exons, and coding exons are indicated by *thick horizontal lines*, *white boxes*, and *black boxes*, respectively. *Bent arrows* indicate ATG start codons, and TAA indicates stop codons. *White arrowheads* above and below the line indicate the insertion and deletion of nucleotides, respectively, and *vertical lines* show nucleotide differences between IRGC105444 and T65 in the genomic region around *mtRPL27*. *Thick black lines* show the positions of the four overlapping clones (NGC1, NGC2, NGC3, and NGC4) containing portions of the *S27-niv*^{s} allele. *Black arrowheads* represent the locations and directions of the primers used for linkage mapping of NGC clones to *S27* in a BC_4F_3 segregating population. **b** Multiple alignments of the predicted amino acid sequences of mtPRL27 proteins from the *S27-T65*$^+$ and *S27-niv*^{s} alleles. *Black background* indicates amino acids conserved among the sequences. *Red asterisk* shows the position of a predicted amino acid difference between the *mtRPL27* genes in *S27-T65*$^+$ and those in *S27-niv*^{s}

we performed the co-segregation analysis of three *S27-niv*^{s} allele-specific dominant markers, *M6_S27*, *M7_S27*, and *M8_S27*, with *RM1309*, which is tightly linked to the *S27* locus (Fig. 1e). In the BC_4F_3 population, T65 homozygotes and heterozygotes at *RM1309* segregated in a 19:28 ratio ($\chi^2 = 1.72$, $P = 0.19$) (Table 3). None of the plants scored as homozygous for the T65 allele of *RM1309* were positive for *M6_S27* and *M8_S27* markers, and all of the plants scored as heterozygous were also positive for *M6_S27* and *M8_S27* markers (Table 3). For *M7_S27* marker, the amplification of the 217 bp DNA fragments from *S27-niv*^{s} allele was positive for the heterozygous plants at *RM1309* whereas the amplification of the 217 bp DNA fragments was not observed for the T65 homozygous plants at *RM1309* (Tables 3, S1). This result demonstrates that the three *S27-niv*^{s} allele-specific dominant markers co-segregated with *RM1309*, indicating the NGC clones were amplified from the *S27* locus.

Table 3 Segregation of genotypes in the BC_4F_3 population, classified by PCR markers

Marker	Segregation for *RM1309* marker					
	TT[a]		TN		NN	
	+[b]	–	+	–	+	–
M6_S27	0	19	28	0	0	0
M7_S27	0	19	28	0	0	0
M8_S27	0	19	28	0	0	0

[a] TT, TN, and NN represent T65 homozygous DNA, heterozygous T65/IRGC105444 DNA, and IRGC105444 homozygous DNA at *RM1309*, respectively

[b] + and – symbols indicate the presence and absence of *S27-niv*^{s} allele-specific DNA bands amplified with *M6_S27*, *M7_S27*, and *M8_S27* markers

Sequence analysis of the NGC clones revealed that copies of both *mtRPL27a* and *mtRPL27b* exist in IRGC105444, although a number of nucleotide mutations were found in the coding and promoter regions of *mtRPL27a* and *mtRPL27b* of *S27-niv*^{s} relative to those of *S27-T65*$^+$ (Fig. 4a). When compared with the predicted mtRPL27a amino acid sequence from *S27-T65*$^+$, the predicted mtRPL27a amino acid sequence from *S27-niv*^{s} showed one amino acid substitution (methionine and isoleucine) in the C-terminal region (Fig. 4b). The mtRPL27b protein sequence predicted from *S27-niv*^{s} had this same substitution. The *mtRPL27a* and *mtRPL27b* at *S27* originated from the *mtRPL27a* at *S28* (Ueda et al. 2006) and both the mtRPL27a proteins deduced from *S28-T65*^{s} and *S28-glum*$^+$ have a methionine residue at the 142nd position (Yamagata et al. 2010). Therefore, the ancestral residue of the 142nd position of the mtRPL27a and mtRPL27b proteins could be methionine. This substitution is not located in the ribosomal protein L27 domain, so it is unknown whether these amino acid substitutions are associated with the defect of the *mtRPL27a* and *mtRPL27b* genes in *S27-niv*^{s}. Although we cannot confirm the causal mutation with this sequence information alone, these mutations found in *S27-niv*^{s} might be the cause of loss-of-function of the *S27-niv*^{s} allele.

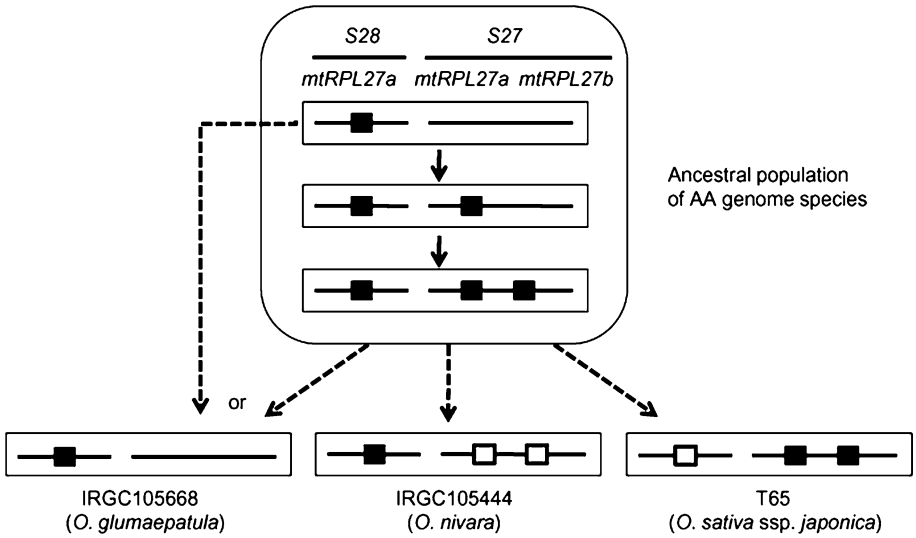

Fig. 5 Model for evolution of loss-of-function alleles of *S27* and *S28* during the process of AA-genome divergence. *Black boxes* and *white boxes* indicate functional genes and pseudogenes, respectively. *Black arrows* represent the duplication of *mtRPL27* genes inferred from the reference sequence of Nipponbare. *Dotted arrows* indicate the speculated origin of loss-of-function alleles *S27-glum*^{s}, *S27-niv*^{s}, and *S28-T65*^{s}. *Rounded rectangle* indicates evolutionary process of duplication of the *mtRPL27* postulated by Ueda et al. (2006)

Discussion

We recently reported that epistatic interaction between *S27* on chromosome 8 and *S28* on chromosome 4 caused hybrid pollen sterility in a cross between T65 and *O. glumaepatula*, and that the *S27-glum*^{s} allele is a loss-of-function allele caused by complete absence of the *mtRPL27a* and *mtRPL27b* genes (Yamagata et al. 2010). Here, we identified a novel loss-of-function allele of *S27*, *S27-niv*^{s}, in hybrids between T65 and *O. nivara* accession IRGC105444. Molecular cloning of the genomic DNA sequence of *S27-niv*^{s} indicated that two tandem copies of *mtRPL27* (*mtRPL27a* and *mtRPL27b*) are located at *S27-niv*^{s}. In addition, a number of nucleotide mutations were found in the coding and promoter regions of *mtRPL27a* and *mtRPL27b* of *S27-niv*^{s} compared with those of *S27-T65*$^+$. These results demonstrate that *S27-niv*^{s} and *S27-glum*^{s} are different loss-of-function alleles at the locus encoding the mtRPL27 protein.

From these results, we propose a model for the evolution of the loss-of-function allele at *S27* in the divergence of AA-genome species (Fig. 5). The analysis of the Nipponbare reference sequences revealed the location of three copies of *mtRPL27*: *mtRPL27a* and *mtRPL27b* at *S27* (chromosome 8) and *mtRPL27a* at *S28* (chromosome 4) (Ueda et al. 2006). *mtRPL27a* at *S28* is the most ancestral locus. An interchromosomal duplication generated a new copy, *mtRPL27a*, at *S27* on chromosome 8, and a subsequent intrachromosomal duplication of *mtRPL27a* at *S27* generated one more copy, *mtRPL27b*, also at *S27* (Ueda et al. 2006). Moreover, because all investigated accessions of the Asian AA-genome rice species (*O. sativa*, *O. nivara*, and *O. rufipogon*) have the duplicated segment at *S27*, we propose that the gene duplication of *mtRPL27a* between *S27* and *S28* occurred in the ancestral progenitor of the Asian wild species (Yamagata et al. 2010). Since the genomic sequences of both *mtRPL27a* and *mtRPL27b* were observed in *S27-niv*^{s}, we propose that loss-of-function events occurred in both *mtRPL27a* and *mtRPL27b* after the intrachromosomal duplication of *mtRPL27* to evolve the sterile allele of *S27-niv*^{s} (Fig. 5). On the other hand, we considered two possibilities for the origin of the *S27-glum*^{s} allele. One is that the allele was directly transmitted from the ancestral genome before the interchromosomal duplication. The other is that it lost both *mtRPL27* copies after the interchromosomal and intrachromosomal duplication events by deletion of the duplicated region. The *S27-glum*^{s} allele was not found in the Asian wild and cultivated rice accessions, although it was found in the African wild species *O. barthii* and *O. longistaminata* (Yamagata et al. 2010). This situation shows that different loss-of-function alleles are distributed in geographically and phylogenetically isolated species and serve as a potential factor of postzygotic isolation in each species. The segmental genomic duplication of *mtRPL27* that occurred in the ancestor of the AA-genome species provided a source of loss-of-function alleles and may have played an important role in the evolution of postzygotic reproductive isolation in the multiple divergent lineages of AA-genome species. Future surveys of other AA-genome accessions should reveal additional types of loss-of-function alleles.

The evolutionary model of hybrid incompatibility by gene duplication and reciprocal losses of duplicated gene function has been proposed as a passive source of postzygotic reproductive isolation between diverged species (Lynch and Force 2000). This model was recently supported by studies of intraspecific hybrids within *A. thaliana* (Bikard et al. 2009) and interspecific hybrids in rice (Yamagata et al. 2010). It is well known that modern plant genomes reflect the frequent occurrence of earlier genomic segmental duplications and polyploidization events; for example, up to 90% of loci are duplicated in *A. thaliana*

and 62% in rice (Paterson et al. 2004; Moore and Purugganan 2005). The duplication of genes followed by loss of function of some of these duplicates may provide a mechanism for gene evolution, enabling postzygotic reproductive isolation in divergent species. Our study provides experimental evidence that the independent evolution of loss-of-function alleles of duplicate genes contributes to postzygotic reproductive isolation.

Acknowledgments This work was supported by a grant from the Ministry of Agriculture, Forestry and Fisheries of Japan (Genomics for Agricultural Innovation, QTL-5002).

References

Allard RW (1956) Formulas and tables to facilitate the calculation of recombination values in heredity. Hilgardia 24:235–278

Bikard D, Patel D, Mette CL, Giorgi V, Camilleri C, Bennett MJ, Loudet O (2009) Divergent evolution of duplicate genes leads to genetic incompatibilities within *A. thaliana*. Science 323:623–626

Chang MT, Neuffer MG (1989) Maize microsporogenesis. Genome 32:232–244

Chen J, Ding J, Ouyang Y, Du H, Yang J, Cheng K, Zhao J, Qiu S, Zhang X, Yao J, Liu K, Wang L, Xu C, Li X, Xue Y, Xia M, Ji Q, Lu J, Xu M, Zhang Q (2008) A triallelic system of *S5* is a major regulator of the reproductive barrier and compatibility of *indica–japonica* hybrids in rice. Proc Natl Acad Sci USA 105:11436–11441

Coyne JA, Orr HA (2004) Speciation. Sinauer Associates, Sunderland, MA

Dellaporta SL, Wood J, Hicks JB (1983) A plant DNA minipreparation: Version II. Plant Mol Biol Rep 1:19–21

Doi K, Yasui H, Yoshimura A (2008) Genetic variation in rice. Curr Opin Plant Biol 11:144–148

Fuse T, Sasaki T, Yano M (2001) Ti-plasmid vectors useful for functional analysis of rice genes. Plant Biotechnol 18:219–222

Heslop-Harrison J, Heslop-Harrison Y (1970) Evaluation of pollen viability by enzymatically induced fluorescence; intercellular hydrolysis of fluorescein diacetate. Strain Tech 45:115–120

Hiei Y, Ohta S, Komari T, Kumashiro T (1994) Efficient transformation of rice (*Oryza sativa* L.) mediated by *Agrobacterium* and sequence analysis of the boundaries of the T-DNA. Plant J 6:271–282

Khush GS (1997) Origin, dispersal, cultivation and variation of rice. Plant Mol Biol 35:25–34

Koide Y, Onishi K, Kanazawa A, Sano Y (2008) Genetics of speciation in rice. In: Hirano H-Y, Hirai A, Sano Y, Sasaki T (eds) Rice biology in the genomics era, biotechnology in agriculture and forestry 62. Springer, Berlin, pp 247–259

Kosambi D (1944) The estimation of map distance from recombination values. Ann Eugen 12:172–175

Long Y, Zhao L, Niu B, Su J, Wu H, Chen Y, Zhang Q, Guo J, Zhuang C, Mei M, Xia J, Wang L, Wu H, Liu YG (2008) Hybrid male sterility in rice controlled by interaction between divergent alleles of two adjacent genes. Proc Natl Acad Sci USA 105:18871–18876

Lynch M, Conery JS (2000) The evolutionary fate and consequences of duplicate genes. Science 290:1151–1155

Lynch M, Force AG (2000) The origin of interspecific genomic incompatibility via gene duplication. Am Nat 156:590–605

McCouch SR, Teytelman L, Xu Y, Lobos KB, Clare K, Walton M, Fu B, Maghirang R, Li Z, Xing Y, Zhang Q, Kono I, Yano M, Fjellstrom R, DeClerck G, Schneider D, Cartinhour S, Ware D, Stein L (2002) Development and mapping of 2240 new SSR markers for rice (*Oryza sativa* L.). DNA Res 9:199–207

Moore RC, Purugganan MD (2005) The evolutionary dynamics of plant duplicate genes. Curr Opin Plant Biol 8:122–128

Oka HI (1988) Functions and genetic basis of reproductive barriers. In: Origin of cultivated rice. Japan Scientific Societies Press/Elsevier, Tokyo, pp 181–209

Paterson AH, Bowers JE, Chapman BA (2004) Ancient polyploidization predating divergence of the cereals, and its consequences for comparative genomics. Proc Natl Acad Sci USA 101:9903–9908

Rieseberg LH, Willis JH (2007) Plant speciation. Science 317:910–914

Sun S, Ting C-T, Wu C-I (2004) The normal function of a speciation gene, *Odysseus*, and its hybrid sterility effect. Science 305:81–83

Ueda M, Arimura S, Yamamoto MP, Takaiwa F, Tsutsumi N, Kadowaki K (2006) Promoter shuffling at a nuclear gene for mitochondrial RPL27. Involvement of interchromosome and subsequent intrachromosome recombinations. Plant Physiol 141:702–710

Win KT, Kubo T, Miyazaki Y, Doi K, Yamagata Y, Yoshimura A (2009) Identification of two loci causing F_1 pollen sterility in inter- and intraspecific crosses of rice. Breed Sci 59:411–418

Yamagata Y, Yamamoto E, Aya K, Win KT, Doi K, Sobrizal, Ito T, Kanamori H, Wu J, Matsumoto T, Matsuoka M, Ashikari M, Yoshimura A (2010) Mitochondrial gene in the nuclear genome induces reproductive barrier in rice. Proc Natl Acad Sci USA 107:1494–1499